Is there an optimal ENSO pattern that increases U.S. tornado activity?

Sang-Ki Lee[1,2], David Enfield[1,2], Hailong Liu[1,2], Chunzai Wang[2], Robert Atlas[2], and Brian Mapes[3]

[1]Cooperative Institute for Marine and Atmospheric Studies, University of Miami, Miami, Florida, USA

[2]Atlantic Oceanographic and Meteorological Laboratory, NOAA, Miami Florida, USA

USA

[3]Rosenstiel School of Marine and Atmospheric Science, University of Miami, Miami, Florida, USA

Submitted to Geophysical Research Letters

June 2011

Corresponding author address: Dr. Sang-Ki Lee, NOAA/AOML, 4301 Rickenbacker Causeway, Miami, FL 33149, USA. E-mail: Sang-Ki.Lee@noaa.gov.

Abstract

Observations and modeling experiments are used to show that a positive phase of Trans-Niño, characterized by cooling in the central tropical Pacific and warming in the eastern tropical Pacific, is linked to an increased number of intense U.S. tornadoes in spring. The warming in the eastern tropical Pacific increases convection locally, but also contributes to suppressing convection in the central tropical Pacific. This in turn works constructively with cooling in the central tropical Pacific to force a strong and persistent negative phase Pacific – North American (PNA)-like teleconnection pattern. The anomalous winds that are associated with this teleconnection pattern bring more cold and dry upper-level air from the high-latitudes and more warm and moist lower-level air from the Gulf of Mexico converging into the central U.S., and thus provide a favorable condition for increased U.S. tornado activity. A distinctive feature in the 2011 Trans-Niño event is warming in the western tropical Pacific that further aided to suppress convection in the central tropical Pacific and thus contributed to strengthening the teleconnection response in the central U.S. in favor of increased U.S. tornado activity.

1. Introduction

In April and May of 2011, a record breaking 1,243 tornadoes were reported in the United States. This resulted in 517 tornado related fatalities, making 2011 one of the deadliest tornado years in U.S. history [http://www.spc.noaa.gov/climo/torn/fataltorn.html]. Questions were raised almost immediately as to whether the series of extreme tornado outbreaks in 2011 could be linked to long-term climate changes. The severe weather database (SWD) from the National Oceanic and Atmospheric Administration indicates that the number of total U.S. tornadoes (i.e., from F0 to F5 in the Fujita-Pearson scale) during the most active tornado months of April and May (AM) has been steadily increasing since 1950 (Figure S1a). However, due to the improvements in tornado detection technology with time, one must be cautious in attributing this secular increase in the number of U.S. tornadoes to a specific long-term climate signal [Brooks and Doswell, 2001]. Since intense and long-lived tornadoes are much more likely to be detected and reported even before a national network of Doppler radar was build in the 1990s, the number of intense U.S. tornadoes (i.e., from F3 to F5 in the Fujita-Pearson scale) in AM during 1950-2010 is obtained from the SWD (Figure S1b) and used, after detrending, as the primary diagnostic index in this study (Figure S1c).

In the central U.S. east of the Rocky Mountains, cold and dry upper-level air from the high latitudes often converges with warm and moist lower-level air coming from the Gulf of Mexico (GoM). Due to this so-called large-scale differential advection (i.e., two or more different air masses converging at different heights), a conditionally unstable atmosphere with high convective available potential energy is formed that causes frequent and intense thunderstorms. With the addition of a triggering mechanism, such as the horizontal spinning effect provided by the lower-level wind shear (i.e., wind speed increasing or wind direction changing with height),

these thunderstorms can spawn intense tornadoes. Consistently, the moisture transport from the GoM to the central U.S. is significantly correlated with the number of intense U.S. tornadoes in AM (see Table 1). See Rasmussen and Blanchard [1998], and Brooks et al. [2003] for various meteorological indices, which are used to estimate the occurrence of tornadoes.

The Pacific – North American (PNA) pattern in boreal winter and spring is linked to the large-scale differential advection in the central U.S. as discussed in earlier studies [e.g., Munoz and Enfield, 2011]. During a negative phase of the PNA, an anomalous cyclone is formed over North America that bring more cold and dry upper-level air from the high latitudes to the central U.S., and an anomalous anticyclone is formed over the southeastern seaboard that increases the southwesterly wind from the GoM to the central U.S., thus enhancing the Gulf-to-U.S. moisture transport. Although the PNA is a naturally occurring atmospheric phenomenon driven by intrinsic variability of the atmosphere, a La Niña in the tropical Pacific can project onto a negative phase PNA pattern [e.g., Lau 1981; Wallace and Gutzler 1981; Straus and Shukla 2002]. In addition, since the Gulf-to-U.S. moisture transport can be enhanced with a warmer GoM, the sea surface temperature (SST) anomaly in the GoM can also affect U.S. tornado activity. During the decay phase of La Niña in spring, the GoM is typically warmer than usual [e.g., Alexander and Scott 2002]. Therefore, the Gulf-to-U.S. moisture transport could be increased during the decay phase of La Niña in spring due to the increased SSTs in the GoM and the strengthening of the southwesterly wind from the GoM to the U.S. Nevertheless, none of these (i.e., PNA, GoM SST, and La Nina) are significantly correlated with the number of intense tornadoes in AM (see Table 1) as discussed in earlier studies [e.g., Cook and Schaefer, 2008]. Currently, seasonal forecast skill for intense U.S. tornado outbreaks, such as occurred in 2011, has not been demonstrated.

Among the long-term climate patterns considered in Table 1, only the Trans-Niño (TNI) is significantly correlated (r = 0.33) with the number of intense U.S. tornadoes in AM. The TNI, which is defined as the difference in normalized SST anomalies between the Niño-1+2 (10S° - 0°; 90°W - 80°W) and Niño-4 (5°N - 5°S; 160°E - 150°W) regions, represents the evolution of the El Niño-Southern Oscillation (ENSO) in the months leading up to the event and the subsequent evolution with opposite sign after the event [Trenberth and Stepaniak, 2001]. Given that AM is typically characterized with the development or decay phase of ENSO events, it is more likely that the tropical Pacific SST anomalies in AM are better represented by the TNI index than the conventional ENSO indices such as Niño-3.4 (5°N - 5°S; 170°W - 120°W) or Niño-3 (5°N - 5°S; 150°W-90°W). Nevertheless, it is not at all clear why the number of intense U.S. tornadoes in AM is significantly correlated with the TNI index, but not with other ENSO indices. This is the central question that we explore in the following sections by using both observations and an atmospheric general circulation model (AGCM).

2. Observations

To better understand the potential link between the TNI and U.S. tornado activity, we ranked the years from 1950 to 2010 (61 years in total) based on the number of intense U.S. tornadoes in AM. The top ten years are characterized by increased Gulf-to-U.S. moisture transport in the lower-level (Figure 1a) and an anomalous upper-level cyclone over North America that advects more cold and dry air to the central U.S. (Figure 1c), whereas the bottom ten years are associated with decreased Gulf-to-U.S. moisture transport (Figure 1b) and an anomalous upper-level anticyclone over North America (Figure 1d). This is consistent with the notion that springtime U.S. tornado activity is modulated by the large-scale differential advection in the central U.S.

Among the top ten years (Table S1), seven years including the top three are identified with a positive phase (i.e., above ¼ quantile) TNI index (i.e., normalized SST anomalies are larger in the Niño-1+2 than in Niño-4 region). Five out of those seven years are characterized by a La Niña transitioning to a different phase or persisting beyond AM (1957, 1965, 1974, 1999, and 2008) and the other two with an El Niño transitioning to either a La Nina or neutral phase (1983 and 1998). Figure 2a shows the composite SST anomalies for those five positive phase TNI years transitioning from a La Niña.

On the other hand, among the bottom ten years (Table S2), only one year is identified with a positive phase TNI, and the other nine years are with a neutral phase (i.e., between ¼ and ¾ quantile) TNI, suggesting that a negative phase of the TNI does not either decrease or increase the number of intense U.S. tornadoes in AM. Interestingly, four years among the bottom ten years are identified with a La Niña transitioning to a different phase or persisting beyond AM (1950, 1951, 1955 and 2001), and four are with an El Niño transitioning to a different phase or persisting beyond AM (1958, 1987, 1988 and 1992). As shown in Figure 2b, the composite SST anomaly pattern for the four years of the bottom ten years with a La Niña transitioning is that of a typical La Niña with the SST anomalies in the Niño-4 and Niño-1+2 being both strongly negative (i.e., neutral phase TNI). Similarly, as shown in Figure 2c, the composite SST anomaly pattern for the four years in the bottom ten years with an El Niño transitioning is that of a typical El Niño with the SST anomalies in the Niño-4 and Niño-1+2 being both strongly positive (i.e., neutral phase TNI).

In summary, observations indicate that a positive phase TNI (i.e., normalized SST anomalies are larger in the Niño-1+2 than in Niño-4 region) is linked to an increased number of intense U.S. tornadoes in AM, whereas both La Niñas and El Niños with a neutral phase TNI (i.e., the

SST anomalies in the Niño-1+2 region are as strong and the same sign as the SST anomalies in the Niño-4) are linked to a decreased number of intense U.S. tornadoes in AM.

3. Model Experiments

To explore the potential link between the three tropical Pacific SST anomaly patterns (see Figure 2), identified in the previous section, and the number of intense U.S. tornadoes in AM, a series of AGCM experiments are performed by using version 3.1 of the NCAR community atmospheric model coupled to a slab mixed layer ocean model (CAM3). The model is a global spectral model with a triangular spectral truncation of the spherical harmonics at zonal wave number 42 (T42). It is vertically divided into 26 hybrid sigma-pressure layers. Model experiments are performed by prescribing various composite evolutions of SSTs in the tropical Pacific region (15°S–15°N; 120°E-coast of the Americas) while predicting the SSTs outside the tropical Pacific using the slab ocean model. To prevent discontinuity of SST around the edges of the forcing region, the model SSTs of three grid points centered at the boundary are determined by combining the simulated and prescribed SSTs. Each ensemble consists of ten model integrations that are initialized with slightly different conditions to represent intrinsic atmospheric variability. The same methodology was previously used in Lee et al. [2008] for studying ENSO teleconnection to the tropical North Atlantic region.

Four sets of ensemble runs are performed (Table S3). In the first experiment (EXP_CLM), the SSTs in the tropical Pacific region are prescribed with climatological SSTs. In the second experiment (EXP_TNI), the composite SSTs of the positive phase TNI years identified among the ten most active U.S. tornado years are prescribed in the tropical Pacific region. Note that only the five positive TNI years transitioning from a La Niña (1957, 1965, 1974, 1999, and 2008) are

considered here because the other two positive TNI years are transitioning from an El Niño (1983 and 1998) and thus tend to cancel the tropical SST anomalies of the other five. In the next two experiments, the SSTs in the tropical Pacific region are prescribed with the composite SSTs of the four years in the bottom ten years with a La Niña transitioning (1950, 1951, 1955 and 2001) for EXP_LAN, and the four years in the bottom ten years with an El Niño transitioning (1958, 1987, 1988 and 1992) for EXP_ELN.

4. Model Results

Figure 3 and S2 show the difference in moisture transport, and geopotential height and wind at 500 hPa in AM obtained by subtracting those fiedls in EXP_CLM from the three model experiments. In EXP_TNI (Figure 3), the Gulf-to-U.S. moisture transport is greatly increased and an anomalous upper-level cyclone is formed over North America that brings more cold and dry air to the central U.S., all indicating enhanced large-scale differential advection in the central U.S. In EXP_LAN and EXP_ELN (Figure S2), on the other hand, the Gulf-to-U.S. moisture transport is neither increased nor decreased. A relatively weak anomalous upper-level cyclone is formed in EXP_LAN, but it is positioned over the eastern seaboard. In EXP_ELN, a weak anomalous upper-level anticyclone is formed and also positioned over the eastern seaboard.

Therefore, these model results fully support the hypothesis that a positive phase of the TNI with cooling in the central tropical Pacific (CP) and warming in the eastern tropical Pacific (EP) enhances the large-scale differential advection in the central U.S. advecting more cold and dry upper-level air from the high-latitudes and more warm and moist lower-level from the GoM, and thus increasing U.S. tornado activity in spring. However, the model results do not show any increase or decrease in the large-scale differential advection in the central U.S. under La Niña

and El Niño conditions as long as the SST anomalies in EP are as strong and the same sign as the SST anomalies in CP.

5. CP- versus EP-forced Teleconnection

The model results strongly suggest that cooling in CP and warming in EP may have a constructive influence on the teleconnection pattern that strengthens the large-scale differential advection over the central U.S. One possibility is that the Rossby wave train forced by warming in EP may have the same spatial structure as that forced by cooling in CP but shifted eastward with the sign reversed. The two linearly independent Rossby wave trains may be superimposed on each other in such a way as to enhance the large-scale differential advection over the central U.S. Such a mechanism is partially supported by the simple two-level dry atmosphere model [Lee et al. 2009] forced with cooling in CP and warming EP (not shown).

To better understand how the real atmosphere with moist diabatic processes responds to CP cooling and EP warming, two sets of additional model experiments (EXP_CPC and EXP_EPW) are performed (Table S3). These two experiments are basically identical to EXP_TNI except that the composite SSTs of the positive phase TNI years are prescribed only in the western and central tropical Pacific region (15°S–15°N; 120°E - 110°W) for EXP_CPC and only in the eastern tropical Pacific region (15°S–15°N; 110°W-coast of the Americas) for EXP_EPW.

Figure 4 show the difference in moisture transport, and geopotential height and wind at 500 hPa in AM obtained by subtracting those fields in EXP_CLM from the two additional model experiments. In EXP_CPC, the teleconnection pattern emanating from the tropical Pacific consists of an anticyclone over the Aleutian Low in the North Pacific, a cyclone over North America, and an anticyclone over the southeastern U.S. and central Americas, consistent with a

typical negative phase PNA pattern (Figure 4c). As expected from the anomalous anticyclone over the southeastern U.S. and central Americas, the Gulf-to-U.S. moisture transport is increased in EXP_CPC (Figure 4b).

Surprisingly, the Rossby wave train forced by warming in EP (EXP_EPW) is very similar to that in EXP_CPC (Figure 4f). Consistently, the Gulf-to-U.S. moisture transport is also increased in EXP_EPW as in EXP_CPC and EXP_TNI (Figure 4e). The teleconnection pattern in EXP_EPW is not either shifted eastward or its sign reversed from that in EXP_CPC. Obviously, a question arises as to why the teleconnection pattern forced by warming in EP is virtually the same as that forced by cooling in CP (see Figure 4c and 4f). It appears that the Rossby wave train in EXP_EPW is not directly forced from EP. In EXP_EPW, convection is increased locally in EP, but it is decreased in CP as in EXP_CPC (Figure S3c). This suggests that increased convection in EP associated with the increased local SSTs suppresses convection in CP that in turn forces a negative phase PNA-like pattern. Therefore, these model results confirm that cooling in CP and warming in EP do have constructive influence on the teleconnection pattern that strengthens the large-scale differential advection over the central U.S. The model results also suggest that cooling in CP with neutral SST anomalies in EP or warming in EP with neutral SST anomalies in CP can strengthen the large-scale differential advection over the central U.S.

An apparently important question is why warming in EP does not directly excite a Rossby wave train to the high-latitudes. As shown in earlier theoretical studies, the vertical background wind shear is one of the two critical factors, which are required for tropical heating to radiate barotropic teleconnections to the high-latitudes [e.g., Lee et al. 2009]. In both observations and EXP_CLM, the background vertical wind shear between 200 and 850 hPa in AM is largest in the central tropical North Pacific and smallest in EP and the western tropical Pacific (WP), providing

an explanation as to why the Rossby wave train in EXP_EPW is not directly forced in EP (Figure S4). See Lee et al. [2009] and references therein for more discussions on this issue.

6. Effect of Intrinsic Variability

The conclusion so far is that a positive phase TNI with cooling in CP and warming in EP can increase U.S. tornado activity in spring because CP cooling and EP warming have constructive influence on the teleconnection pattern that strengthens the large-scale differential advection over the central U.S. However, the correlation between the TNI and the number of intense U.S. tornadoes in AM is only 0.33 indicating that the TNI can explain only about 10% of the total variance. This suggests that intrinsic variability in the atmosphere may overwhelm the TNI-teleconnection pattern over North America as discussed in earlier studies for El Niño-teleconnection patterns in the Pacific–North American region [e.g., Hoerling and Kumar, 1997]. In order to better illustrate this point, we select neutral TNI years during 1950-2010 and divide them into one group with an increased Gulf-to-U.S. moisture transport in AM and the other group with a decreased Gulf-to-U.S. moisture transport. Figure S5b shows the difference in moisture transport between these two groups. Similarly, we divide ten ensemble experiments for EXP_CLM into two groups, one with an increased Gulf-to-U.S. moisture transport in AM and the other group with a decreased Gulf-to-U.S. moisture transport. Figure S5c shows the difference in moisture transport between these two groups.

As expected, the typical amplitude of Gulf-to-U.S. moisture transport induced by intrinsic variability in the atmosphere such as the PNA during neutral phase TNI years is larger than the anomalous Gulf-to-U.S. moisture transport for positive phase TNI years (Figure S5a). Similarly, internal variability in EXP_CLM can generate anomalous Gulf-to-U.S. moisture transport with

comparable amplitude to that simulated in EXP_TNI. Therefore, we can conclude that the strengthening of the large-scale differential advection over the central U.S. during a positive phase of the TNI can be greatly reduced or enhanced by internal variability in the atmosphere. In other words, although seven of the ten most active tornado years during 1950-2010 including the top three years are characterized with a strongly positive phase of the TNI (Table S1), the associated predictability of U.S. tornado activity, which can be defined as a ratio of the climate signal (the TNI index in this case) relative to the climate noise, is low.

7. U.S. Tornado Outbreaks in 2011

A positive phase of the TNI prevailed during AM of 2011 with cooling in CP and warming EP (Figure S6a). An important question is whether the series of extreme U.S. tornado outbreaks during AM of 2011 can be attributed to this positive of the TNI. During AM of 2011, an anomalous upper-level anticyclone was formed over North America (Figure S6c), and the Gulf-to-US moisture was greatly increased (Figure S6b), both indicating the coherent teleconnection response to a positive phase of the TNI. To confirm this, a set of model experiments (EXP_011) is performed by prescribing the SSTs for 2010 - 2011 in the tropical Pacific region while predicting the SSTs outside the tropical Pacific using the slab ocean model (Table S3). As summarized in Figure S7, the model results are consistent with the observations, although the anomalous Gulf-to-US moisture is weaker in the model experiment.

A distinctive feature in the 2011 TNI event is warming in WP (Figure S6a). Further experiments (Table S3) suggest that the warming in WP indirectly suppresses convection in CP, and thus works constructively with the cooling in CP to force a strong and persistent negative phase PNA-like pattern (Figure S8 and S9). Thus, despite the low signal-to-noise ratio in the

TNI-teleconnection response in the central U.S., it is highly likely that the 2011 positive phase TNI event did contribute to the increased number of intense U.S. tornadoes in AM of 2011 by enhancing the differential advection in the central U.S.

8. Discussion

The record-breaking U.S. tornado outbreak in the spring of 2011 prompts the need to identify and understand long-term climate signals that provide seasonal predictability for intense tornado outbreaks. Here, we use both observations and modeling experiments to demonstrate that a positive phase of the TNI, characterized by cooling in CP and warming in EP, is one such climate pattern that can strengthen the large-scale differential advection in the central U.S. and thus increase U.S. tornado activity. However, although seven of the ten most active tornado years during 1950 – 2010 including the top three are characterized with a strongly positive phase of the TNI, the TNI explains only 10% of the total variance in the number of intense U.S. tornadoes in AM. Therefore, further study is needed to refine the predictive skill provided by the TNI and to explore other long-term climate signals that can provide additional predictability in seasonal and longer time scales. It is important to point out some limitations in this study. In particular, the atmospheric model used as the main tool in this study (CAM3) has a relatively low-resolution (T42), which may be subject to large model bias. A related issue is that the major results in this study are based on a single-model. Obviously, more rigorous multi-model experiments with various horizontal resolutions are required to test if the major conclusions of this study are not model-dependent. Finally, a potentially important long-term climate signal not explicitly explored in this study is what appears to be a shift in the number of intense U.S. tornadoes in AM around 1980 (Figure S1b). Although it is unclear whether this shift is real or a bias in the

SWD, it is in line with the shift in the Pacific Decadal Oscillation (PDO) phase that occurred around the same time. It is possible that the in-phase combination of ENSO and PDO leads to stronger and more persistent PNA-like teleconnection pattern [e.g., Yu and Zwiers, 2007].

Acknowledgments. This study was motivated and benefited from interactions with scientists at NOAA ESRL, GFDL, CPC, and NCDC. In particular, we wish to thank Wayne Higgins, Tom Karl, Marty Hoerling, and Harold Brooks for initiating and leading discussions that motivated this study. This work was supported by grants from the National Oceanic and Atmospheric Administration's Climate Program Office and by grants from the National Science Foundation.

References

Alexander, M., and J. Scott (2002), The influence of ENSO on air-sea interaction in the Atlantic. *Geophys. Res. Lett*., **29**, 1701. doi:10.1029/2001GL014347.

Brooks, H. E., C. A. Doswell III (2001), Some aspects of the international climatology of tornadoes by damage classification, *Atmos. Res*., **56**, 191– 201.

Brooks, H. E., J. W. Lee, and J. P. Cravenc (2003), The spatial distribution of severe thunderstorm and tornado environments from global reanalysis data, *Atmos. Res*., **67-68**, 73-94.

Cook, A. R., and J. T. Schaefer (2008), The relation of El Niño–Southern Oscillation (ENSO) to winter tornado outbreaks, *Mon. Wea. Rev*., **136**, 3121–3137.

Hoerling, M. P., and A. Kumar (1997), Why do North American climate anomalies differ from one El Niño event to another?, *Geophys. Res. Lett*., **24**, 1059-1062.

Lau, N.-C., and M. J. Nath (2001), Impact of ENSO on SST variability in the North Pacific and North Atlantic: Seasonal dependence and role of extratropical air-sea coupling, *J. Clim.*, **14**, 2846–2866.

Lee, S.-K., D. B. Enfield and C. Wang (2008), Why do some El Ninos have no impact on tropical North Atlantic SST? *Geophys. Res. Lett.*, **35**, L16705, doi:10.1029/2008GL034734.

Lee, S.-K., C. Wang and B. E. Mapes (2009), A simple atmospheric model of the local and teleconnection responses to tropical heating anomalies. *J. Clim.*, **22**, 272-284.

Munoz, E., and D. Enfield (2010), The boreal spring variability of the Intra-Americas low-level jet and its relation with precipitation and tornadoes in the eastern United States, *Clim. Dyn*. **36**, 247–259.

Rasmussen, E. N., D. O. Blanchard (1998), A baseline climatology of sounding-derived supercell and tornado forecast parameters. *Weather Forecast.* **13**, 1148–1164.

Straus, D. M., and J. Shukla (2002), Does ENSO force the PNA?, *J. Clim.*, **15**, 2340–2358.

Trenberth, K. E., and D. P. Stepaniak (2001), Indices of El Niño evolution, *J. Clim.*, 14, 1697–1701.

Wallace, J. M., and D. S. Gutzler (1981), Teleconnections in the geopotential height field during the Northern Hemisphere Winter, *Mon. Wea. Rev.*, **109**, 784-812.

Yu, B., and F. W. Zwiers (2007), The impact of combined ENSO and PDO on the PNA climate: a 1,000-year climate modeling study, *Clim. Dyn.*, **29**, 837-851.

Table 1. Correlation coefficients of various long-term climate patterns with the number of intense (F3 - F5) tornados in April and May (AM) during 1950-2010. All indices including the tornado index are detrended. The SWD, ERSST3, and NCEP-NCAR reanalysis are used to obtain the long-term climate indices used in this table. Any correlation value with above the 95% significance is in bold[a]

Index	DJF	FMA	AM
Gulf-to-U.S. moisture transport	0.08	0.20	**0.40**
GoM SST	0.15	0.21	0.20
Niño-4	-0.22	-0.20	-0.19
Niño-3.4	-0.13	-0.13	-0.11
Niño-1+2	0.02	0.11	0.15
TNI	**0.28**	**0.29**	**0.33**
PNA	-0.05	-0.10	-0.20
PDO	-0.12	-0.10	-0.14
NAO	-0.01	-0.10	-0.18

[a]The Gulf-to-U.S. meridional moisture transport is obtained by averaging the vertically integrated moisture transport in the region of 25°N - 35°N and 100°W - 90°W. The North Atlantic Oscillation (NAO) index and the Pacific - North American (PNA) pattern are defined as the first and second leading modes of Rotated Empirical Orthogonal Function (REOF) analysis of monthly mean geopotential height at 500 hPa, respectively. The Pacific Decadal Oscillation (PDO) is the leading principal component of monthly SST anomalies in the North Pacific Ocean north of 20°N.

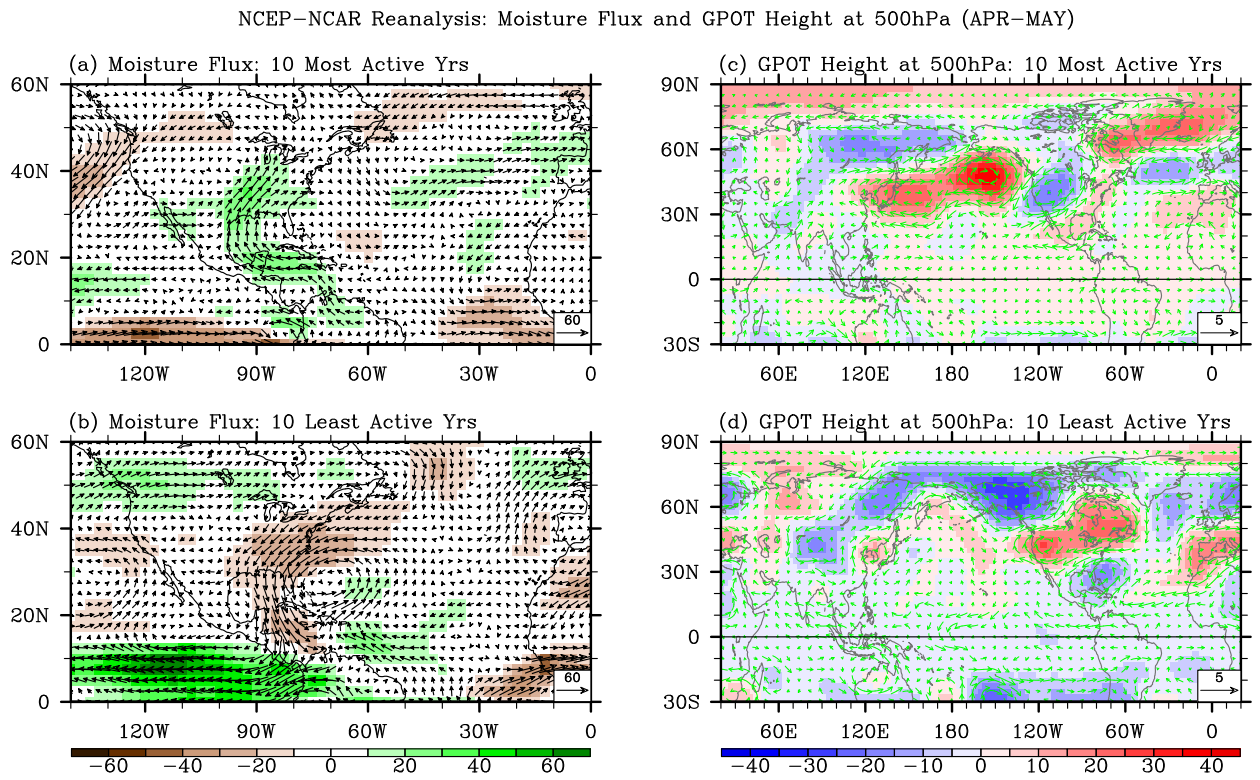

Figure 1. Anomalous moisture transport for (a) the ten most active U.S. tornado years and (b) the ten least active U.S. tornado years in AM during 1950-2010 obtained from NCEP-NCAR reanalysis. Anomalous geopotential height and wind at 500 hPa for (c) the ten most active U.S. tornado years and (d) the ten least active U.S. tornado years in AM during 1950-2010 obtained from NCEP-NCAR reanalysis. The unit is kg $m^{-1}sec^{-1}$ for moisture transport, m for geopotential height, and m s^{-1} for wind.

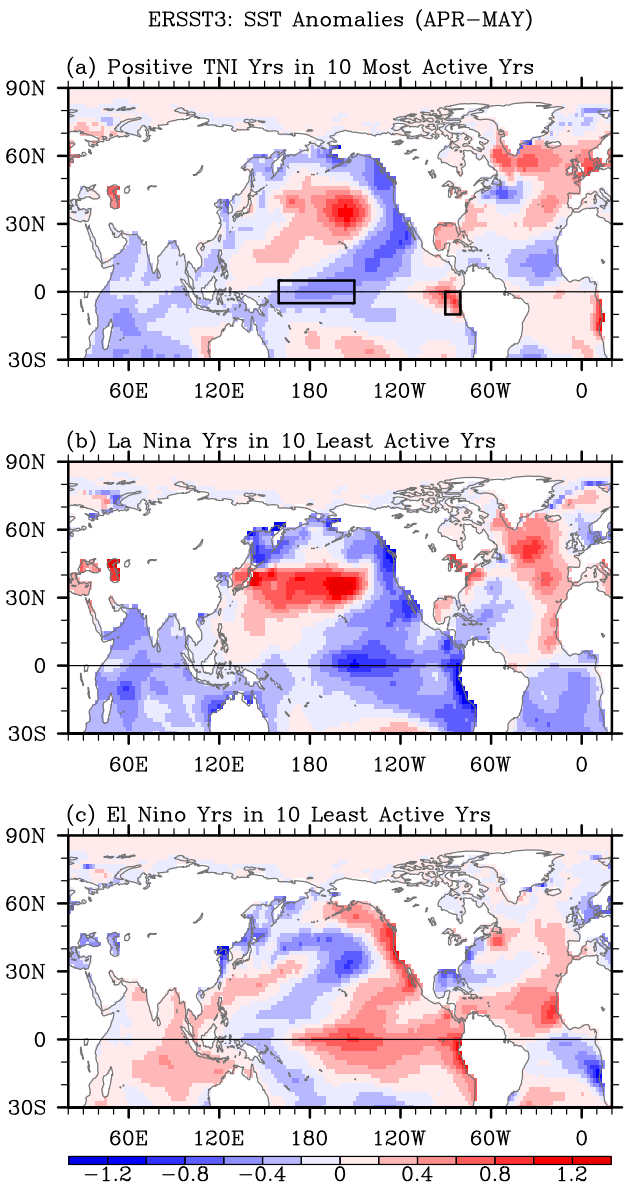

Figure 2. Composite SST anomalies in AM, obtained from ERSST3, for (a) the five positive TNI years transitioning from a La Niña identified among the ten most active U.S. tornado years in AM during 1950-2010, and for (b) the four years with a La Niña transitioning and (c) the four years with an El Niño transitioning identified among the ten least active U.S. tornado years in AM during 1950-2010. Thick black lines in (a) indicate the Niño-4 (5°N - 5°S; 160°E - 150°W) and Niño-1+2 (10S° - 0°; 90°W - 80°W) regions.

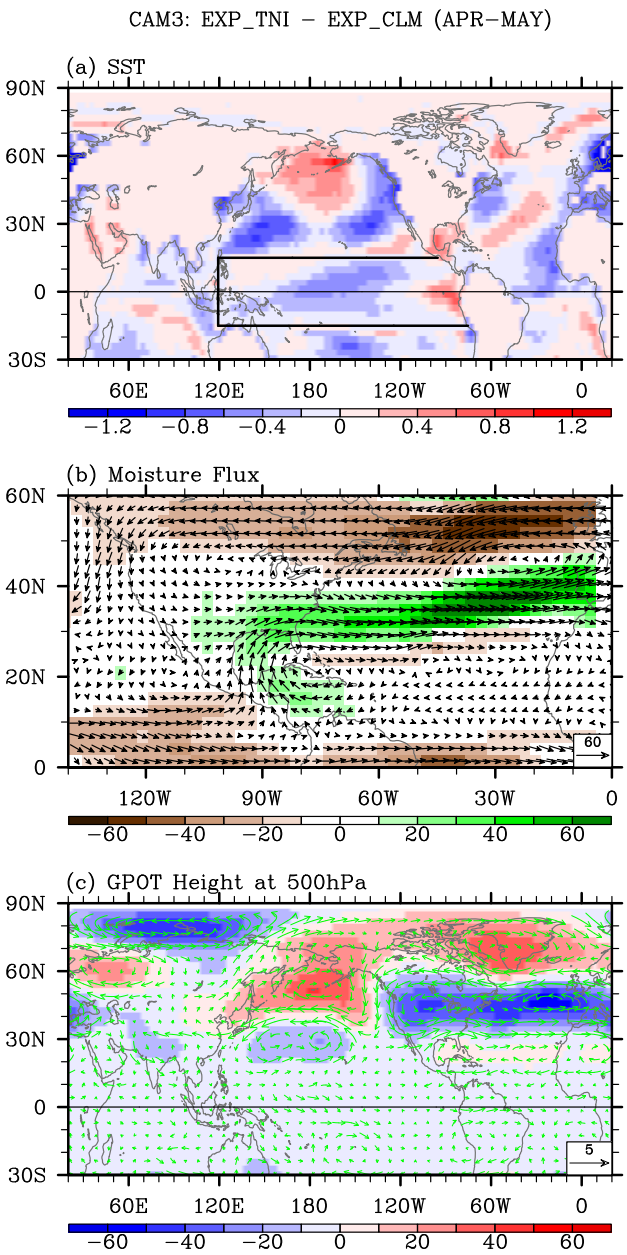

Figure 3. Simulated anomalous (a) SST, (b) moisture transport, and (c) geopotential height and wind at 500 hPa in AM obtained from EXP_TNI – EXP_CLM. The unit is °C for SST, kg m^{-1} sec^{-1} for moisture transport, m for geopotential height, m s^{-1} for wind. Thick black lines in (a) indicate the tropical Pacific region where the model SSTs are prescribed.

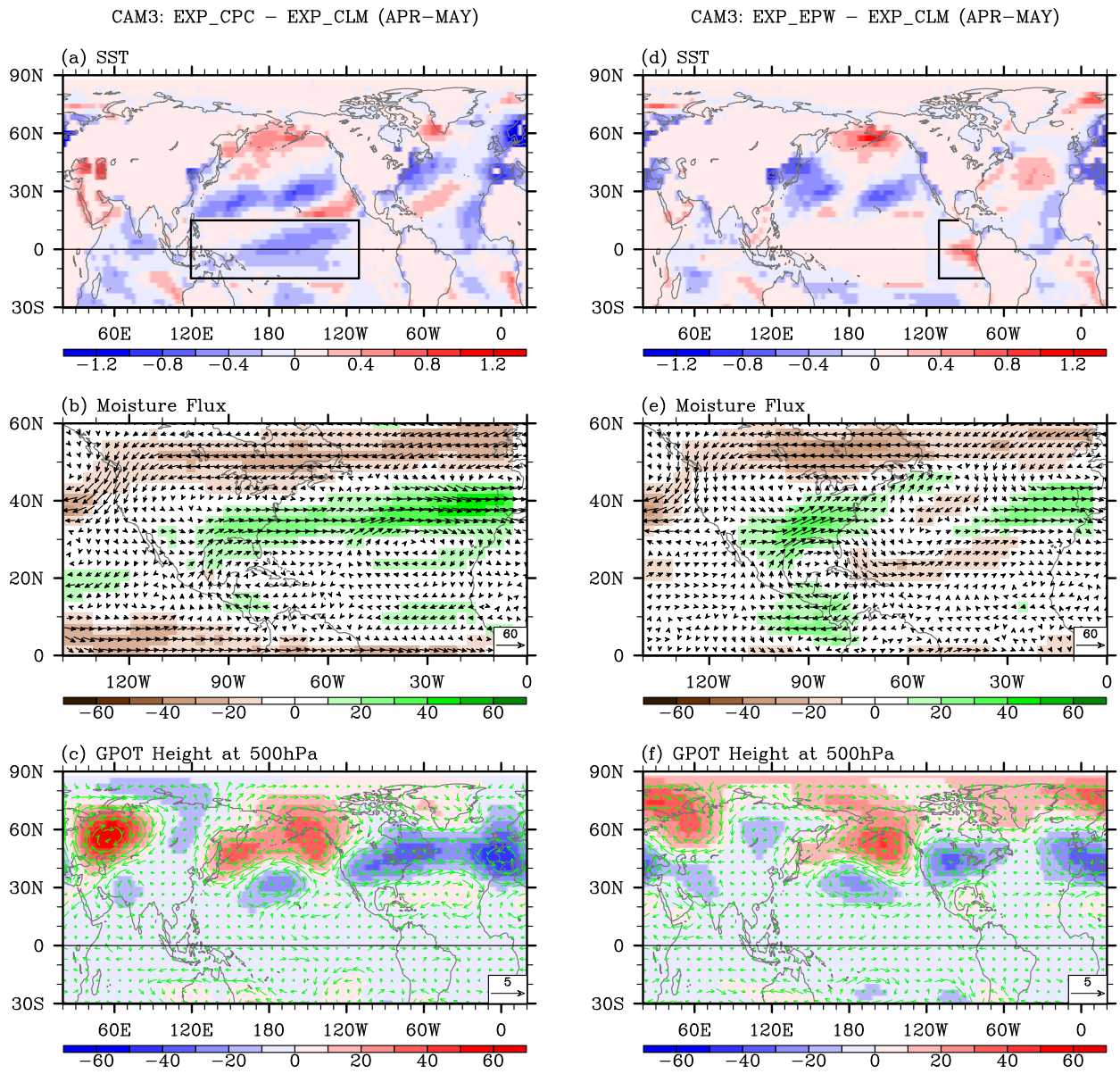

Figure 4. Simulated anomalous (a) SST, (b) moisture transport, and (c) geopotential height and wind at 500 hPa in AM obtained from EXP_CPC – EXP_CLM. Simulated anomalous (d) SST, (e) moisture transport, and (f) geopotential height and wind at 500 hPa in AM obtained from EXP_EPW – EXP_CLM. The unit is °C for SST, kg m^{-1} sec^{-1} for moisture transport, m for geopotential height, and m s^{-1} for wind. Thick black lines in (a) and (d) indicate the regions where the model SSTs are prescribed.

Table S1. The total of 61 years from 1950 to 2010 are ranked based on the detrended number of intense U.S. tornadoes in AM. The top ten most active U.S. tornado years are listed with ENSO phase in spring and TNI index in AM for each year. Strongly positive (above ¼ quantile) and negative (below ¾ quantile) TNI index values are in bold and italic, respectively.

Ranking	Year	ENSO phase in spring	TNI index (detrended)
1	1974	La Niña persists	**1.30 (1.48)**
2	1965	La Niña transitions to El Niño	**1.39 (1.54)**
3	1957	La Niña transitions to El Niño	**0.57 (0.69)**
4	1982	El Niño develops	*-1.11* (*-0.89*)
5	1973	El Niño transitions to La Niña	-0.42 (-0.24)
6	1999	La Niña persists	**0.47 (0.75)**
7	1983	El Niño decays	**1.86 (2.08)**
8	2003	El Niño decays	*-1.24* (*-0.94*)
9	2008	La Niña decays	**1.41 (1.73)**
10	1998	El Niño transitions to La Niña	**1.69 (1.97)**

Table S2. The total of 61 years from 1950 to 2010 are ranked based on the detrended number of intense U.S. tornadoes in AM. The bottom ten years are listed with ENSO phase in spring and TNI index in AM for each year. Strongly positive (above ¼ quantile) and negative (below ¾ quantile) TNI index values are in bold and italic, respectively.

Ranking	Year	ENSO phase in spring	TNI index (detrended)
52	1958	El Niño decays	-0.61 (-0.49)
53	1955	La Niña persists	-0.27 (-0.16)
54	2001	La Niña decays	0.21 (0.50)
55	1986	El Niño develops	-0.39 (-0.16)
56	1988	El Niño transitions to La Niña	-0.37 (-0.13)
57	1987	El Niño persists	0.10 (0.34)
58	1992	El Niño decays	0.21 (0.47)
59	1952	Neutral	-0.67 (-0.57)
60	1951	La Niña transitions to El Niño	-0.31 (-0.22)
61	1950	La Niña persists	**0.77 (0.86**)

Table S3. Prescribed SSTs in the tropical Pacific region for each model experiment. All model experiments are initiated from April of the prior year to December of the modeling year. For instance, in EXP_TNI, the model is integrated for 21 months starting in April using the composite April SSTs of 1956, 1964, 1973, 1998, and 2007.

Experiments	Prescribed SSTs in the tropical Pacific region
EXP_CLM	Climatological SSTs are prescribed in the tropical Pacific region (15°S–15°N; 120°E-coast of the Americas).
EXP_TNI	Composite SSTs of the five positive phase TNI years transiting from a La Niña identified among the ten most active U.S. tornado years (1957, 1965, 1974, 1999, and 2008) are prescribed in the tropical Pacific region.
EXP_LAN	Composite SSTs of the four years with a La Niña transitioning (1950, 1951, 1955 and 2001) identified among the ten least active U.S. tornado years are prescribed in the tropical Pacific region.
EXP_ELN	Composite SSTs of the four years with an El Niño transitioning (1958, 1987, 1988 and 1992) identified among the ten least active U.S. tornado years are prescribed in the tropical Pacific region
EXP_CPC	Same as EXP_TNI except that during that during the modeling year the composite SSTs are prescribed only in the western and central tropical Pacific region (15°S–15°N; 120°E - 110°W).
EXP_EPW	Same as EXP_TNI except that during the modeling year composite SSTs are prescribed only in the eastern tropical Pacific region (15°S–15°N; 110°W-coast of the Americas).
EXP_011	SSTs for 2010-2011 are prescribed in the tropical Pacific region.
EXP_WPW	Same as EXP_011 except that during that during the modeling year SSTs for 2010-2011 are prescribed only in the western Pacific region (15°S–15°N; 120°E - 180°).

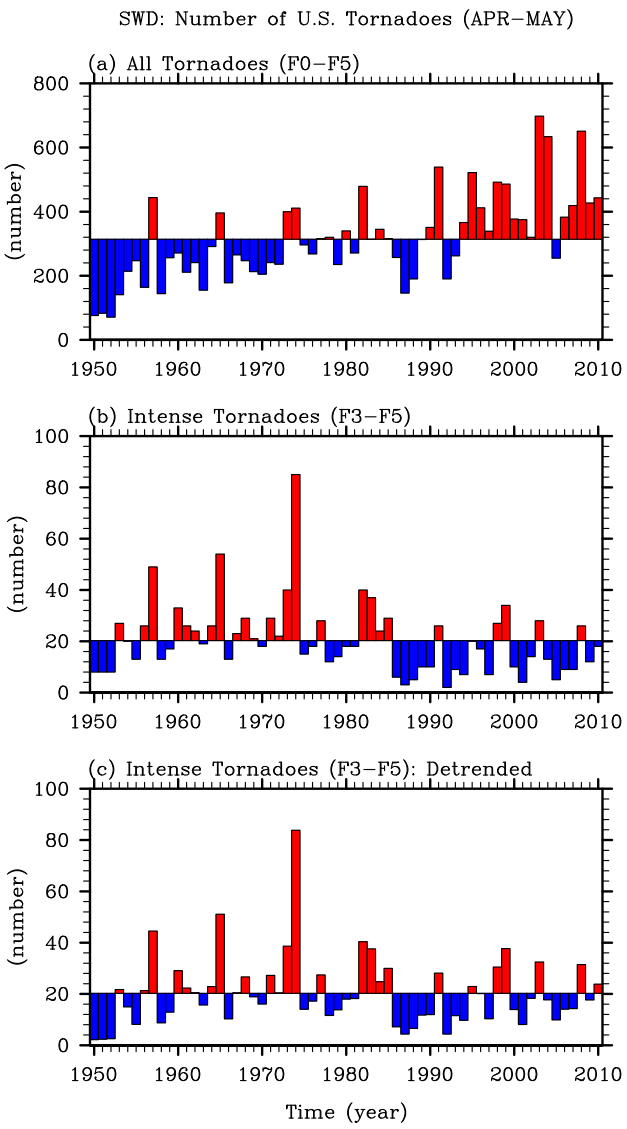

Figure S1. The number of (a) total (F0 – F5) and (b) intense (F3 – F5) US tornadoes for the most active tornado months of April and May (AM) during 1950-2010 obtained from SWD. The detrended number of intense U.S. tornadoes in AM, which is the primary diagnostic index used in this study, is shown in (c).

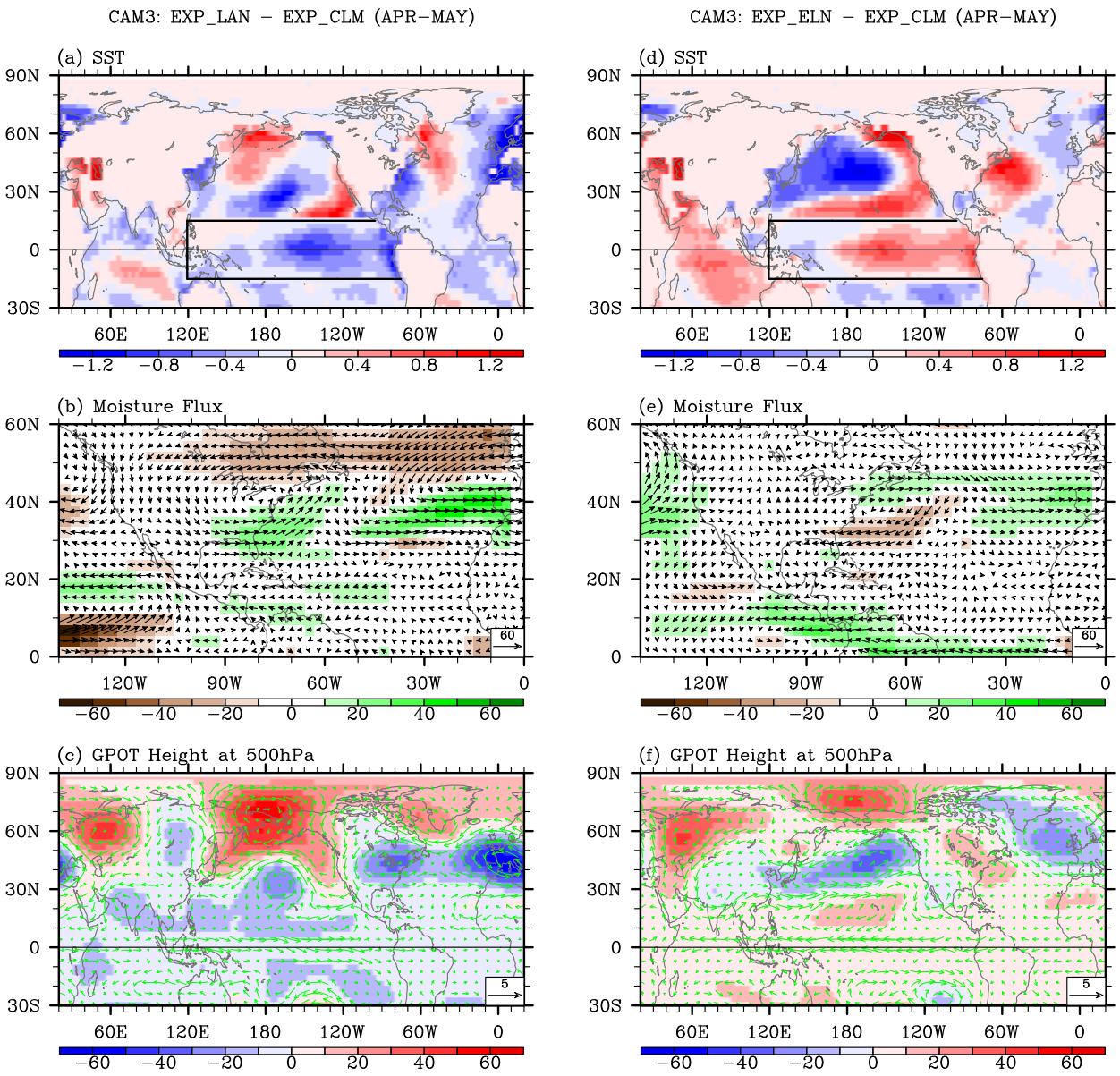

Figure S2. Simulated anomalous (a) SST, (b) moisture transport, and (c) geopotential height and wind at 500 hPa in AM obtained from EXP_LAN – EXP_CLM. Simulated anomalous (d) SST, (e) moisture transport, and (f) geopotential height and wind at 500 hPa in AM obtained from EXP_ELN – EXP_CLM. The unit is °C for SST, kg m^{-1} sec^{-1} for moisture transport, m for geopotential height, and m s^{-1} for wind. Thick black lines in (a) and (d) indicate the tropical Pacific region where the model SSTs are prescribed.

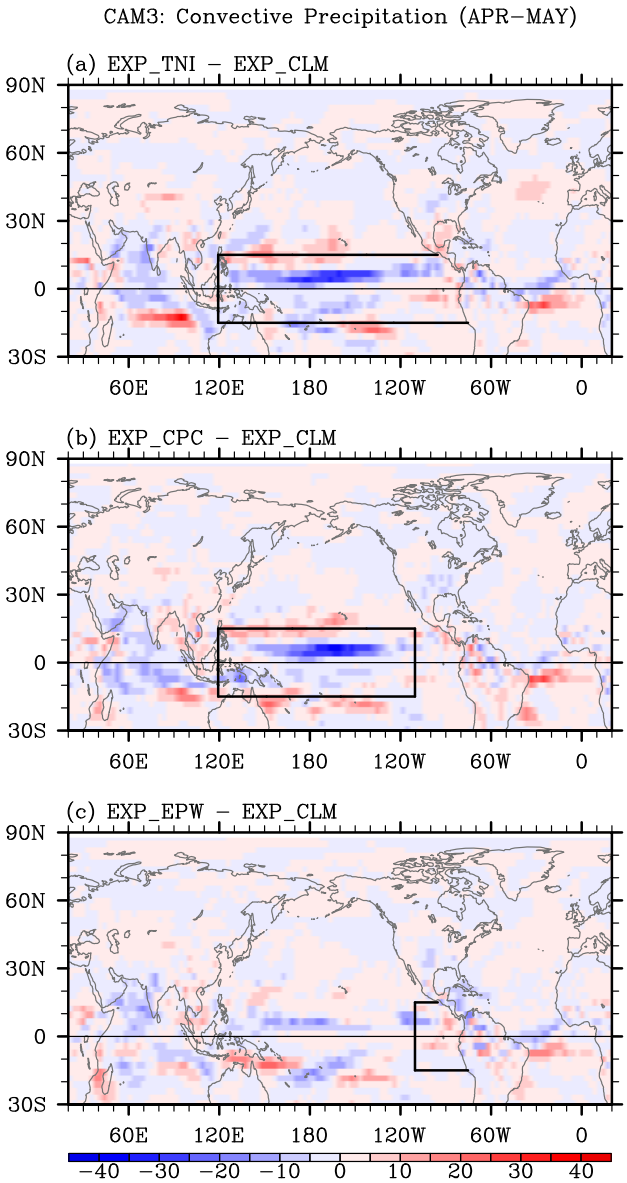

Figure S3. Simulated anomalous convective precipitation rate in AM obtained from (a) EXP_TNI – EXP_CLM, (b) EXP_CPC – EXP_CLM, and (c) EXP_EPW – EXP_CLM. The unit is mm day^{-1}.

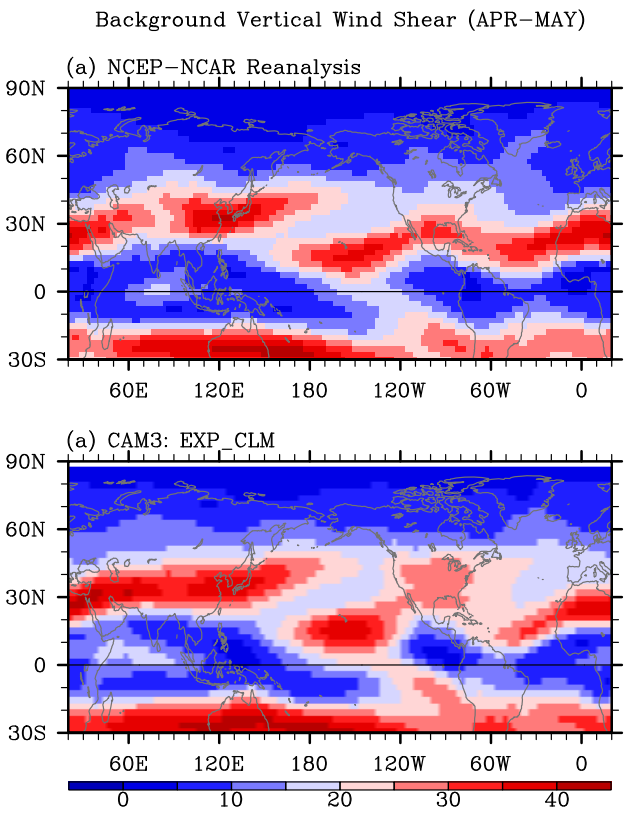

Figure S4. Background (climatological) vertical wind shear between 200 and 850 hPa in AM obtained from (a) NCEP-NCAR reanalysis, and (b) EXP_CLM. The unit is m sec $^{-1}$.

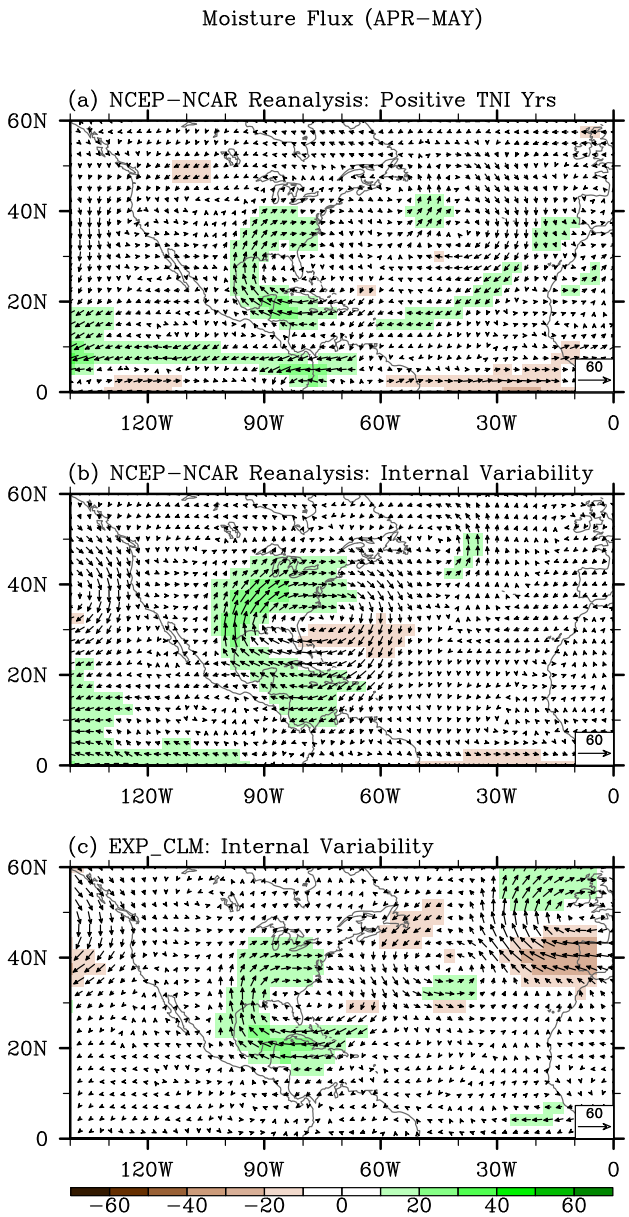

Figure S5. (a) Anomalous composite moisture transport for positive (above ¼ quantile) TNI years during 1950-2010. Neutral TNI years during 1950-2010 are divided into one group with increased Gulf-to-US moisture transport in AM and the other group with decreased Gulf-to-US moisture transport. (b) The difference in moisture transport between these two groups obtained from NCEP-NCAR reanalysis. Similarly, ten ensemble experiments for EXP_CLM are divided into two groups, one with increased Gulf-to-US moisture transport in AM and the other group with decreased Gulf-to-US moisture transport. (c) The difference in moisture transport between these two groups derived from EXP_CLM. The unit is kg m^{-1} sec^{-1}.

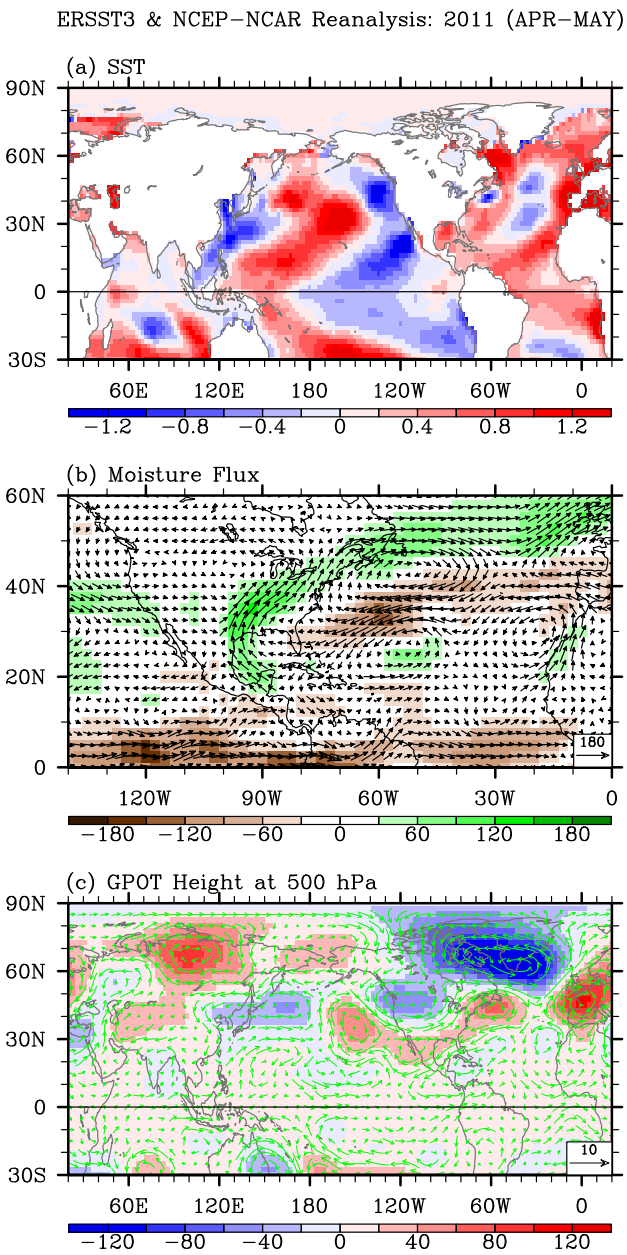

Figure S6. Anomalous (a) SST, (b) moisture transport, and (c) geopotential height and wind at 500 hPa in AM of 2011. The SST is obtained from ERSST3. The moisture transport, geopotential height, and wind are obtained from NCEP-NCAR reanalysis. The unit is °C for SST, kg m^{-1} sec^{-1} for moisture transport, m for geopotential height, and m s^{-1} for wind.

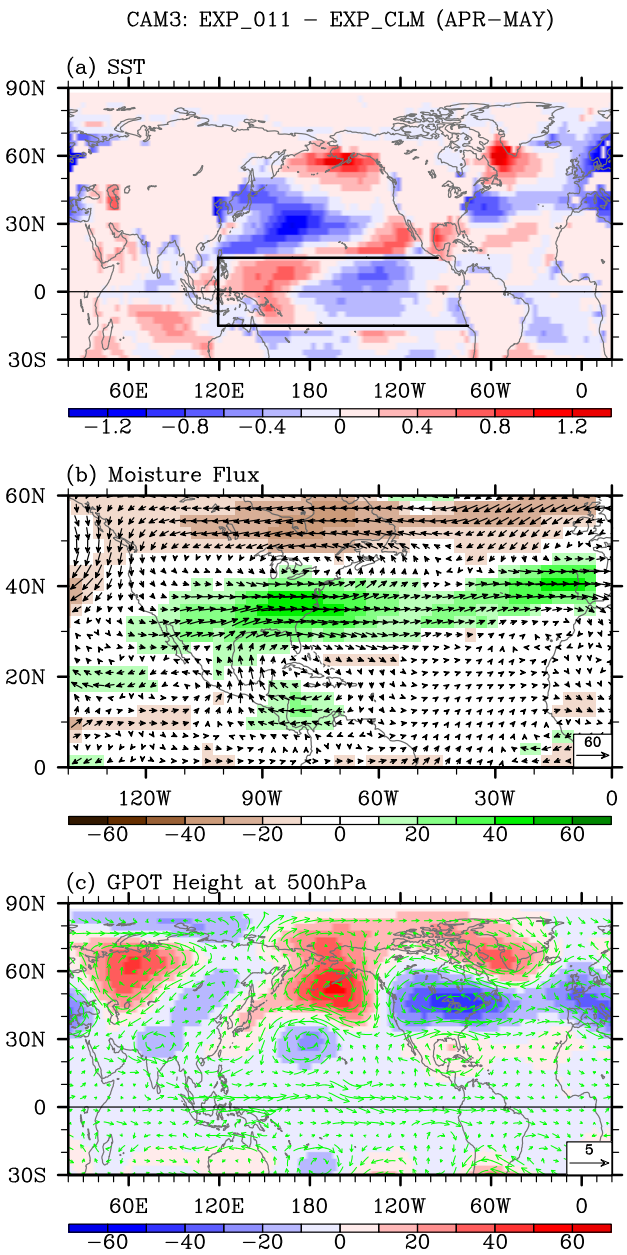

Figure S7. Simulated anomalous (a) SST, (b) moisture transport, and (c) geopotential height and wind at 500 hPa in AM obtained from EXP_011 – EXP_CLM. The unit is °C for SST, kg m^{-1} sec^{-1} for moisture transport, m for geopotential height, m s^{-1} for wind. Thick black lines in (a) indicate the tropical Pacific region where the model SSTs are prescribed.

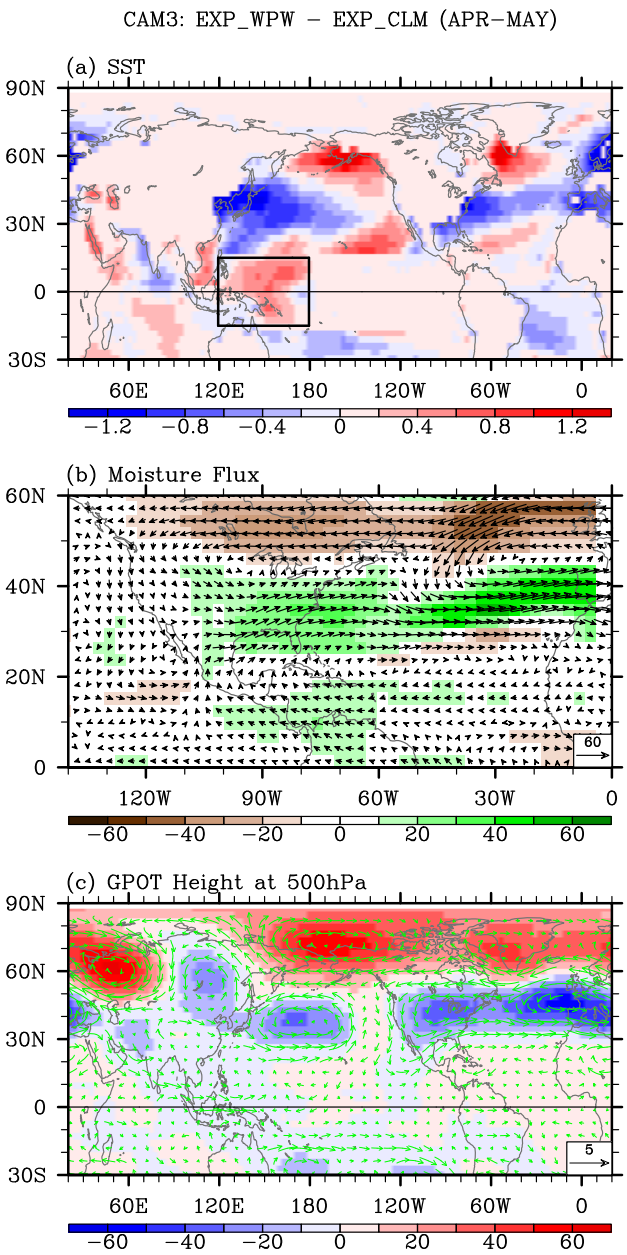

Figure S8. Simulated anomalous (a) SST, (b) moisture transport, and (c) geopotential height and wind at 500 hPa in AM obtained from EXP_WPW – EXP_CLM. The unit is °C for SST, kg m^{-1} sec^{-1} for moisture transport, m for geopotential height, m s^{-1} for wind. Thick black lines in (a) indicate the western Pacific region where the model SSTs are prescribed.

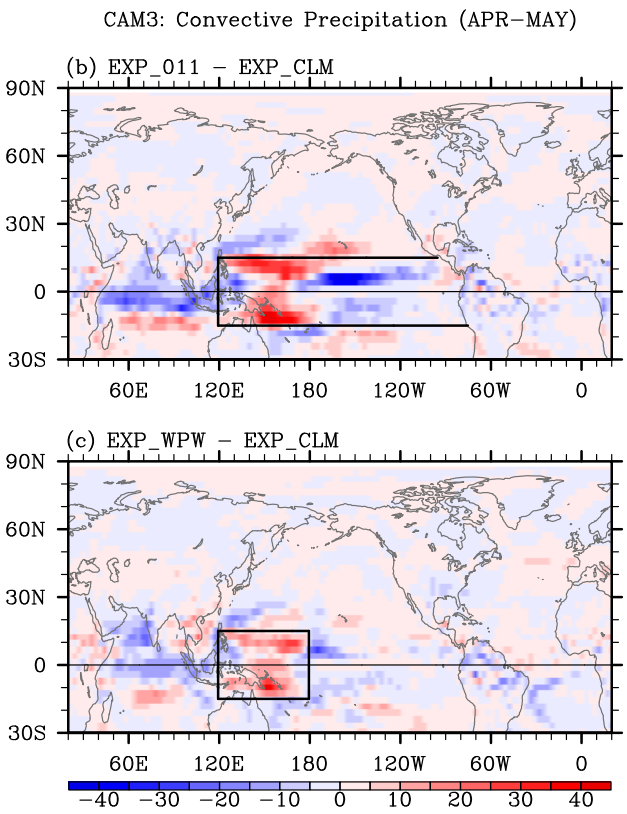

Figure S9. Simulated anomalous convective precipitation rate in AM obtained from (a) EXP_011 – EXP_CLM, and (b) EXP_WPW – EXP_CLM. The unit is mm day^{-1}.